A complex variable boundary element method for axisymmetric heat conduction in a nonhomogeneous solid

W. T. Ang* and B. I. Yun
Division of Engineering Mechanics
School of Mechanical and Aerospace Engineering
Nanyang Technological University
Singapore 639798

Abstract

A complex variable boundary element method is proposed for solving numerically the axisymmetric steady-state problem of heat conduction in a nonhomogeneous isotropic solid. To assess the validity and the accuracy of the method, it is applied to solve specific cases of the problem. The numerical solutions obtained agree well with known solutions.

Keywords: complex variable boundary element method, axisymmetric heat conduction, nonhomogeneous solids.

This is a preprint of an article that has been accepted for publication in the journal *Applied Mathematics and Computation.* When the article is published, it may be access through the following link:
http://dx.doi.org/10.1016/j.amc.2011.07.039.

* Author for correspondence (W. T. Ang)
E-mail: mwtang@ntu.edu.sg
http://www.ntu.edu.sg/home/mwtang/

1 Introduction

The boundary element method is one of the earliest mesh reduction numerical techniques for solving boundary value problems. It requires only the boundary of the solution domain to be discretized into elements. During the last few decades, the method has been used to solve a wide range of problems in engineering and physical sciences. Some examples of works on the boundary element method are Ang and Clements [2] (fracture mechanics), Ang *et al* [3] (nonhomogeneous media), Brebbia and Dominguez [4] (potential problems), Brebbia and Nardini [5] (dual-reciprocity boundary element method), Chen and Hong [9] (dual boundary element formulation), Clements *et al* [7] (anisotropic elasticity), Hong and Chen [11] (hypersingular formulation), Ooi *et al* [13] (bioheat analysis) and Rizzo [15] (isotropic elasticity).

The Cauchy integral formula in the theory of complex functions may be applied to derive boundary element procedures for plane problems. Such a complex variable boundary element approach for solving numerically the two-dimensional Laplace's equation was apparently introduced by Hromadka and Lai [12]. Park and Ang [14] extended the method to an elliptic partial differential equation with variable coefficients. The treatment of the flux boundary conditions in [14], however, differed from that in [12]. In Park and Ang [14] as well as in Chen and Chen [8], the flux boundary conditions were approximated by discretizing a differentiated form of the Cauchy integral formula.

Recently, Dobroskok and Linkov [10] devised a complex variable boundary element method for solving numerically a two-dimensional transient diffusion problem. The time derivative of the unknown function in the diffusion equation was approximated using radial basis functions to reformulate the problem as one governed by the two-dimensional Laplace's equation. The Laplace's equation was then solved by constructing numerically a suitable complex function. A similar complex variable boundary element technique

was given by Ang [1] for the numerical solution of the partial differential equation governing the two-dimensional steady-state heat conduction in a nonhomogeneous anisotropic solid.

In this paper, the complex variable boundary element approach is further developed to solve the problem of axisymmetric steady-state heat conduction in a nonhomogeneous isotropic solid. Guided by the analysis in [1] and [10], we use suitable interpolating functions to approximate certain terms in the governing partial differential equation, in order to reduce the problem to constructing an appropriate analytic complex function. The complex variable boundary element procedure presented here should provide a useful and interesting alternative to the axisymmetric boundary integral method in Brebbia *et al* [6] and Yun and Ang [16], which requires the computation of a rather complicated fundamental solution that is expressed in terms of complete elliptic integrals of the first and second kind. To assess the validity and the accuracy of the numerical procedure presented here, it is applied to solve some specific cases of the axisymmetric heat conduction problem.

2 An axisymmetric heat conduction problem

Consider a thermally isotropic solid occupying the three-dimensional region R. If T is the steady-state temperature inside the solid, then the conservation of energy and the classical Fourier's law of heat conduction require that the temperature to satisfy the partial differential equation

$$\nabla \bullet (\kappa \nabla T) + Q = 0 \text{ in } R, \tag{1}$$

where ∇ is the gradient (nabla) operator, $\bullet$ denotes the dot product, κ is the thermal conductivity and Q is the internal heat source generation rate.

Referring to a Cartesian coordinate system denoted by $Oxyz$, we assume that the geometry of the region R is symmetrical about the z-axis, that is, the boundary of R can be obtained by rotating a curve on the Oxz plane

by an angle of 360° about the z-axis. Moreover, if r and θ denote the polar coodinates defined by $x = r\cos\theta$ and $y = r\sin\theta$, the temperature and the internal heat source generation rate are assumed to be independent of θ, given by $T(r,z)$ and $Q(r,z)$ respectively. The thermal conductivity is functionally graded in the radial and axial directions of the solid of revolution, that is,

$$\kappa = g(r,z), \tag{2}$$

where g is a suitably given function that is positive in R.

Of interest here is the numerical solution of (1) together with (2) subject to the boundary conditions

$$\begin{aligned} T(r,z) &= f_1(r,z) \text{ on } \Xi_1, \\ g(r,z)\frac{\partial T}{\partial n} &= f_2(r,z) + f_3(r,z)T(r,z) \text{ on } \Xi_2, \end{aligned} \tag{3}$$

where Ξ_1 and Ξ_2 are non-intersecting surfaces such that $\Xi_1 \cup \Xi_2 = \Xi$, Ξ is the (surface) boundary of the region R, $\partial T/\partial n$ denotes the outward normal derivative of T on Ξ and $f_1(r,z)$, $f_2(r,z)$ and $f_3(r,z)$ are suitably given functions of r and z.

If we let

$$T(r,z) = \frac{1}{\sqrt{g(r,z)}} w(r,z), \tag{4}$$

then (1) can be written as

$$\frac{\partial^2 w}{\partial r^2} + \frac{\partial^2 w}{\partial z^2} = -\frac{Q(r,z)}{\sqrt{g(r,z)}} + B(r,z)w - \frac{1}{r}\frac{\partial w}{\partial r}, \tag{5}$$

where

$$B(r,z) = \frac{1}{\sqrt{g(r,z)}} \nabla^2(\sqrt{g(r,z)}), \tag{6}$$

The function g is assumed to be such that $B(r,z)$ is bounded in the solution domain R.

If the region R and its surface boundary Ξ are obtained by rotating respectively the two-dimensional region Ω and the curve C on the rz plane as sketched in Figure 1, then the boundary value problem defined by (1) together with (2) and (3) can be reformulated as one that requires solving (5) subject to

$$\begin{aligned} w(r,z) &= \sqrt{g(r,z)} f_1(r,z) \text{ on } C_1, \\ \frac{\partial}{\partial n}[w(r,z)] &= \frac{1}{g(r,z)}\{\frac{1}{2}\frac{\partial}{\partial n}[g(r,z)] + f_3(r,z)\}w(r,z) \\ &\quad + \frac{1}{\sqrt{g(r,z)}} f_2(r,z) \text{ on } C_2, \end{aligned} \tag{7}$$

where C_1 and C_2 denote the curves (on the rz plane) that can be rotated by an angle of 360^o about the z-axis to generate the surfaces Ξ_1 and Ξ_2 respectively, and

$$\begin{aligned} \frac{\partial}{\partial n}[w(r,z)] &= n_r(r,z)\frac{\partial}{\partial r}[w(r,z)] + n_z(r,z)\frac{\partial}{\partial z}[w(r,z)], \\ \frac{\partial}{\partial n}[g(r,z)] &= n_r(r,z)\frac{\partial}{\partial r}[g(r,z)] + n_z(r,z)\frac{\partial}{\partial z}[g(r,z)], \end{aligned} \tag{8}$$

with $n_r(r,z)$ and $n_z(r,z)$ being the components of the outward unit normal vector on C at the point (r,z) in the r and z direction respectively. Note that Ξ_1 and Ξ_2 are the surfaces mentioned in (3) and C_1 and C_2 are non-intersecting curves on the Orz plane such that $C_1 \cup C_2 = C$.

In Figure 1, C is sketched as an open curve with its endpoints A_0 and A_1 on the z axis. In general, C may possibly be a closed curve, as in, for example, the case in which the solution domain R is a hollow cylindrical region.

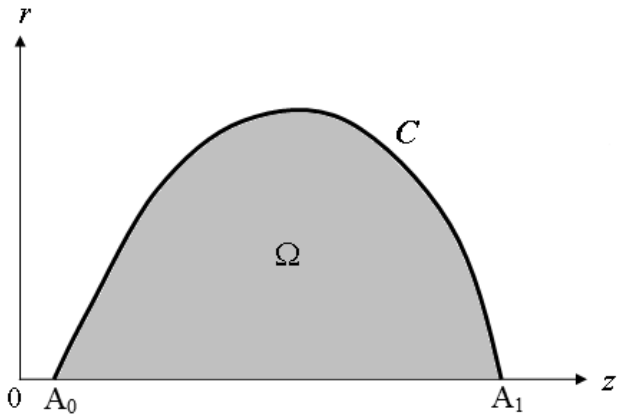

Figure 1. A geometrical sketch of the problem on the rz plane.

3 Interpolating function approximation and complex variable formulation

To approximate the right hand side of (5) using a meshfree approximation, we choose P well spaced out collocation points in $\Omega \cup C$. (The collocation points may lie on $r = 0$ if the solution domain R contains Cartesian points (x, y, z) such that $x^2 + y^2 = 0$.) The collocation points in the axisymmetric coordinates (r, z) are denoted by $(\rho^{(1)}, \zeta^{(1)})$, $(\rho^{(2)}, \zeta^{(2)}), \cdots$, $(\rho^{(P-1)}, \zeta^{(P-1)})$ and $(\rho^{(P)}, \zeta^{(P)})$. We make the approximation

$$-\frac{Q(r,z)}{\sqrt{g(r,z)}} + B(r,z)w - \frac{1}{r}\frac{\partial w}{\partial r} \simeq \sum_{p=1}^{P} \alpha^{(p)} \sigma_1^{(p)}(r,z), \tag{9}$$

where $\alpha^{(p)}$ is a constant coefficient and the interpolating function $\sigma_1^{(p)}(r,z)$ centered about $(\rho^{(p)}, \zeta^{(p)})$ is taken here to be of the form

$$\begin{aligned} \sigma_1^{(p)}(r,z) = &\left([r-\rho^{(p)}]^2 + [z-\zeta^{(p)}]^2\right)^{1/2} \\ &+ \left([r+\rho^{(p)}]^2 + [z-\zeta^{(p)}]^2\right)^{1/2} \end{aligned} \tag{10}$$

As in Yun and Ang [16], we take into consideration the distance between (r, z) and the virtual mirror image of the collocation point $(\rho^{(p)}, \zeta^{(p)})$ about the z axis (that is, the point $(-\rho^{(p)}, \zeta^{(p)})$) in forming the interpolating function in (10), so that the function w_0 in (14) below is such that $\partial w_0/\partial r$ behaves as $O(r)$ for small r. Note that the choice of the interpolating function in (10) is not unique.

We can let (r, z) in (9) be given by $(\rho^{(m)}, \zeta^{(m)})$ for $m = 1, 2, \cdots, P$, to set up a system of linear algebraic equations in $\alpha^{(p)}$. The system can be inverted to obtain

$$\alpha^{(p)} = \sum_{m=1}^{P} \{ -\frac{Q^{(m)}}{\sqrt{g^{(m)}}} + B^{(m)} w^{(m)} - (\frac{1}{r}\frac{\partial w}{\partial r}) \Big|_{(r,z)=(\rho^{(m)},\zeta^{(m)})} \} \chi^{(mp)}, \tag{11}$$

where $w^{(m)} = w(\rho^{(m)}, \zeta^{(m)})$, $B^{(m)} = B(\rho^{(m)}, \zeta^{(m)})$, $Q^{(m)} = Q(\rho^{(m)}, \zeta^{(m)})$, $g^{(m)} = g(\rho^{(m)}, \zeta^{(m)})$ and $\chi^{(mp)}$ are constants defined by

$$\sum_{m=1}^{P} \sigma_1^{(p)}(\rho^{(m)}, \zeta^{(m)}) \chi^{(mr)} = \begin{cases} 1 & \text{if} \quad p = r, \\ 0 & \text{if} \quad p \neq r. \end{cases} \tag{12}$$

Note that the value of $(1/r)\partial w/\partial r$ at $(r, z) = (\rho^{(m)}, \zeta^{(m)})$ must be interpreted in a limiting sense if $\rho^{(m)} = 0$, that is,

$$(\frac{1}{r}\frac{\partial w}{\partial r}) \Big|_{(r,z)=(\rho^{(m)},\zeta^{(m)})} = \lim_{r \to 0^+} (\frac{1}{r}\frac{\partial w}{\partial r}) \Big|_{z=\zeta^{(m)}} \quad \text{if } \rho^{(m)} = 0. \tag{13}$$

Guided by the analysis in Ang [1] and Dobroskok and Linkov [10], for the solution of (5), we write

$$w(r, z) = w_0(r, z) + w_1(r, z) \tag{14}$$

and choose $w_0(r, z)$ to satisfy

$$\frac{\partial^2 w_0}{\partial r^2} + \frac{\partial^2 w_0}{\partial z^2} = -\frac{Q(r, z)}{\sqrt{g(r, z)}} + B(r, z) w - \frac{1}{r}\frac{\partial w}{\partial r}, \tag{15}$$

so that $w_1(r,z)$ is to be obtained by solving

$$\frac{\partial^2 w_1}{\partial r^2}+\frac{\partial^2 w_1}{\partial z^2}=0. \tag{16}$$

From (9), (10) and (11), an approximate solution of (15) may be given by

$$\begin{aligned} w_0(r,z) \simeq \sum_{m=1}^{P} D^{(m)}(r,z)\{-\frac{Q^{(m)}}{\sqrt{g^{(m)}}}+B^{(m)}w^{(m)} \\ -(\frac{1}{r}\frac{\partial w}{\partial r})\Big|_{(r,z)=(\rho^{(m)},\zeta^{(m)})}\}, \end{aligned} \tag{17}$$

where

$$D^{(m)}(r,z)=\sum_{p=1}^{P}\chi^{(mp)}\tau^{(p)}(r,z), \tag{18}$$

and

$$\begin{aligned} \tau^{(p)}(r,z) = \frac{1}{9}([r-\rho^{(p)}]^2+[z-\zeta^{(p)}]^2)^{3/2} \\ +\frac{1}{9}([r+\rho^{(p)}]^2+[z-\zeta^{(p)}]^2)^{3/2}. \end{aligned} \tag{19}$$

To work out a suitable formula for approximating $\partial w/\partial r$ at $(r,z)=(\rho^{(m)},\zeta^{(m)})$, take

$$w(r,z)\simeq\sum_{p=1}^{P}\beta^{(p)}\sigma_2^{(p)}(r,z), \tag{20}$$

where

$$\begin{aligned} \sigma_2^{(p)}(r,z) = \left([r-\rho^{(p)}]^2+[z-\zeta^{(p)}]^2\right)^{5/2} \\ +\left([r+\rho^{(p)}]^2+[z-\zeta^{(p)}]^2\right)^{5/2} \end{aligned} \tag{21}$$

If we let (r, z) in (20) be given by $(\rho^{(m)}, \zeta^{(m)})$ for $m = 1, 2, \cdots, P$ to set up a system of linear algebraic equations in $\beta^{(p)}$, the system can be inverted to obtain

$$\beta^{(p)} = \sum_{m=1}^{P} \eta^{(mp)} w^{(m)}, \tag{22}$$

where

$$\sum_{m=1}^{P} \sigma_2^{(p)}(\rho^{(m)}, \zeta^{(m)}) \eta^{(mr)} = \begin{cases} 1 & \text{if} \quad p = r, \\ 0 & \text{if} \quad p \neq r. \end{cases} \tag{23}$$

From (20) and (22), we obtain the approximation

$$\frac{1}{r}\frac{\partial w}{\partial r} \simeq \sum_{n=1}^{P} L^{(n)}(r, z) w^{(n)}, \tag{24}$$

where

$$L^{(n)}(r, z) = \sum_{p=1}^{P} \eta^{(np)} \frac{1}{r}\frac{\partial}{\partial r}(\sigma_2^{(p)}(r, z)) \text{ for } r > 0. \tag{25}$$

Because of the choice of $\sigma_2^{(p)}(r, z)$ in (21), the function $L^{(n)}(r, z)$ is bounded in the entire region $r > 0$ and it tends to a finite value as $r \to 0^+$. The complex variable boundary element method presented in Section 4 below requires the evaluation of $L^{(n)}(r, z)$ at $r = 0$, if the solution domain R contains points (x, y, z) such that $x^2 + y^2 = 0$. We define $L^{(n)}(0, z)$ as the limit of $L^{(n)}(r, z)$ as $r \to 0^+$. More specifically,

$$\begin{aligned} L^{(n)}(r, 0) = \sum_{p=1}^{P} 10\eta^{(np)} \{ & 3[\rho^{(p)}]^2([\rho^{(p)}]^2 + [z - \zeta^{(p)}]^2)^{1/2} \\ & + ([\rho^{(p)}]^2 + [z - \zeta^{(p)}]^2)^{3/2}\}. \end{aligned} \tag{26}$$

Also, note that the choice of $\sigma_2^{(p)}(r, z)$ in (21) ensures that $w(r, z)$ as approximated in (20) is sufficiently smooth to give a good approximation of

$(1/r)\partial w/\partial r$ at or near $r = 0$. For $w(r,z)$ given by particular functions, numerical experiments indicate that the approximation of $(1/r)\partial w/\partial r$ in (24) near $r = 0$ is quite poor in accuracy if we replace $\sigma_2^{(p)}(r,z)$ in (21) by less smooth interpolating functions such as $\left([r-\rho^{(p)}]^2+[z-\zeta^{(p)}]^2\right)^{3/2}+\left([r+\rho^{(p)}]^2+[z-\zeta^{(p)}]^2\right)^{3/2}$.

With (24), we find that (17) can be rewritten as

$$w_0(r,z) \simeq \sum_{m=1}^{P} D^{(m)}(r,z)\{-\frac{Q^{(m)}}{\sqrt{g^{(m)}}}+B^{(m)}w^{(m)} - \sum_{n=1}^{P} L^{(n)}(\rho^{(m)},\zeta^{(m)})w^{(n)}\}. \tag{27}$$

The general solution of (16) is given by

$$w_1(r,z) = \mathrm{Re}\{F(z+ir)\}, \tag{28}$$

where $i=\sqrt{-1}$ and $F(z+ir)$ is an arbitrary complex function that is analytic in the region Ω on the rz plane.

The boundary condition in (7) can be rewritten as

$$\begin{aligned} & w(r,z) = p_1(r,z) \text{ for } (r,z)\in C_1, \\ & \sum_{m=1}^{P} E^{(m)}(r,z)w^{(m)} + p_3(r,z)\,\mathrm{Re}\{F(z+ir)\} \\ & + \mathrm{Re}\{[n_z(r,z)+in_r(r,z)]F'(z+ir)\} \\ & = p_2(r,z) \text{ for } (r,z)\in C_2, \end{aligned} \tag{29}$$

where the prime denotes differentiation with respect to the relevant argument

and

$$
\begin{aligned}
p_1(r,z) &= \sqrt{g(r,z)}f_1(r,z),\\
p_2(r,z) &= \frac{f_2(r,z)}{\sqrt{g(r,z)}} + \sum_{m=1}^{P}\{G^{(m)}(r,z) + D^{(m)}(r,z)p_3(r,z)\}\frac{Q^{(m)}}{\sqrt{g^{(m)}}},\\
p_3(r,z) &= -\frac{1}{g(r,z)}\{\frac{1}{2}\frac{\partial}{\partial n}[g(r,z)] + f_3(r,z)\},\\
E^{(m)}(r,z) &= B^{(m)}[G^{(m)}(r,z) + D^{(m)}(r,z)p_3(r,z)]\\
&\quad - \sum_{n=1}^{P}[G^{(n)}(r,z) + D^{(n)}(r,z)p_3(r,z)]L^{(m)}(\rho^{(n)},\zeta^{(n)})\\
G^{(m)}(r,z) &= n_r(r,z)\frac{\partial}{\partial r}[D^{(m)}(r,z)] + n_z(r,z)\frac{\partial}{\partial z}[D^{(m)}(r,z)].
\end{aligned}
\tag{30}
$$

If we can construct $F(z+ir)$ that is analytic in Ω and find the constants $w^{(1)}$, $w^{(2)}$, $\cdots$, $w^{(P-1)}$ and $w^{(P)}$ such that (29) is satisfied, then we have approximately solved the boundary value problem stated in Section 2. The required solution of the boundary value problem is then approximately given by

$$
\begin{aligned}
T(r,z) \simeq \frac{1}{\sqrt{g(r,z)}}(&\sum_{m=1}^{P} D^{(m)}(r,z)\{-\frac{Q^{(m)}}{\sqrt{g^{(m)}}} + B^{(m)}w^{(m)}\\
&- \sum_{n=1}^{P} L^{(n)}(\rho^{(m)},\zeta^{(m)})w^{(n)}\} + \mathrm{Re}\{F(z+ir)\}).
\end{aligned}
\tag{31}
$$

4 Complex variable boundary element procedure

According to the Cauchy integral formula, for $(\rho,\zeta)\in\Omega$, we can write

$$
2\pi i F(\zeta+i\rho) = \oint\limits_{(z,r)\in S} \frac{F(z+ir)\,d(z+ir)}{(z-\zeta+i[r-\rho])}, \tag{32}
$$

$$
2\pi i F'(\zeta+i\rho) = \oint\limits_{(z,r)\in S} \frac{F(z+ir)\,d(z+ir)}{(z-\zeta+i[r-\rho])^2}, \tag{33}
$$

where S the curve enclosing the region Ω is assigned the anticlockwise direction.

For the region Ω as sketched in Figure 1 (where the curve C is not a closed curve), the curve S in (32) and (33) comprises C and Γ, where Γ is the portion of the z axis from the point A_0 to A_1. As $\partial T/\partial r$ is expected to be 0 on Γ, we may impose the additional condition:

$$\begin{aligned}&\sum_{m=1}^{P} E^{(m)}(r,z)w^{(m)} + p_3(r,z)\,\mathrm{Re}\{F(z+ir)\}\\&+ \mathrm{Re}\{[n_z(r,z) + in_r(r,z)]F'(z+ir)\}\\&= p_4(r,z) \text{ for } (r,z) \text{ on } \Gamma,\end{aligned} \tag{34}$$

where

$$p_4(r,z) = \sum_{m=1}^{P}\{G^{(m)}(r,z) + D^{(m)}(r,z)p_3(r,z)\}\frac{Q^{(m)}}{\sqrt{g^{(m)}}}. \tag{35}$$

Note that $n_z(r,z) = 0$ and $n_r(r,z) = -1$ for $(r,z) \in \Gamma$. Also, the definition of function $f_3(r,z)$ in $p_3(r,z)$ is extended to include $f_3(r,z) = 0$ for $(r,z) \in \Gamma$.

If C is a closed curve then $S = C$ and (34) is not applicable.

We shall now apply (32) and (33) to devise a procedure for constructing numerically $F(z+ir)$ and finding $w^{(1)}$, $w^{(2)}$, $\cdots$, $w^{(P-1)}$ and $w^{(P)}$ to satisfy the boundary conditions on S. The boundary conditions are given by (29) and 34) (if the latter is applicable).

Put M closely packed points $(r^{(1)}, z^{(1)})$, $(r^{(2)}, z^{(2)})$, $\cdots$, $(r^{(M-1)}, z^{(M-1)})$ and $(r^{(M)}, z^{(M)})$ on the curve S following the anticlockwise direction. For $m = 1, 2, \cdots, M$, define $S^{(m)}$ to be the straight line segment from $(r^{(m)}, z^{(m)})$ to $(r^{(m+1)}, z^{(m+1)})$ (with $(r^{(M+1)}, r^{(M+1)}) = (r^{(1)}, z^{(1)})$). The first M collocation points in (9) and (10) are chosen to be midpoints of $S^{(1)}$, $S^{(2)}$, $\cdots$, $S^{(M-1)}$ and $S^{(M)}$, that is,

$$(\rho^{(m)}, \zeta^{(m)}) = \frac{1}{2}(r^{(m)} + r^{(m+1)}, z^{(m)} + z^{(m+1)}) \text{ for } m = 1, 2, \cdots, M. \tag{36}$$

Another N collocation points given by $(\rho^{(M+1)}, \zeta^{(M+1)})$, $(\rho^{(M+2)}, \zeta^{(M+2)})$, $\cdots$, $(\rho^{(M+N-1)}, \zeta^{(M+N-1)})$ and $(\rho^{(M+N)}, \zeta^{(M+N)})$ are chosen to lie in the interior of Ω. (Thus, the total number of collocation points is given by $P = M + N$.)

Following Park and Ang [14], we make the approximation $S \simeq S^{(1)} \cup S^{(2)} \cup \cdots \cup S^{(M)}$ and discretize the Cauchy integral formula in (32) as

$$2\pi i F(Z) = \sum_{k=1}^{M} (u^{(k)} + iv^{(k)}) \left[\lambda(Z^{(k)}, Z^{(k+1)}, Z) + i\theta(Z^{(k)}, Z^{(k+1)}, Z)\right] \quad \text{for } Z \in \Omega, \tag{37}$$

where $Z = z + ir$, $Z^{(m)} = z^{(m)} + ir^{(m)}$, $u^{(k)}$ and $v^{(k)}$ are real constants given by $u^{(k)} + iv^{(k)} = F(\zeta^{(k)} + i\rho^{(k)})$ and λ and θ are real parameters defined by

$$\begin{aligned}
\lambda(a,b,c) &= \ln|b-c| - \ln|a-c| \\
\theta(a,b,c) &= \begin{cases} \Theta(a,b,c) & \text{if} \quad \Theta(a,b,c) \in (-\pi, \pi] \\ \Theta(a,b,c) + 2\pi & \text{if} \quad \Theta(a,b,c) \in [-2\pi, -\pi] \\ \Theta(a,b,c) - 2\pi & \text{if} \quad \Theta(a,b,c) \in (\pi, 2\pi] \end{cases} \\
\Theta(a,b,c) &= \mathrm{Arg}(b-c) - \mathrm{Arg}(a-c).
\end{aligned} \tag{38}$$

Note that $\mathrm{Arg}(z)$ denotes the principal argument of the complex number z. If the solution domain Ω is convex in shape, $\theta(a,b,c)$ can be calculated directly from

$$\theta(a,b,c) = \cos^{-1}\left(\frac{|b-c|^2 + |a-c|^2 - |b-a|^2}{2\,|b-c|\,|a-c|}\right). \tag{39}$$

If we let $Z \to \widehat{Z}^{(k)} = \zeta^{(k)} + i\rho^{(k)}$ (for each of the collocation points), the imaginary part of (37) gives

$$u^{(k)} = \frac{1}{2\pi} \sum_{m=1}^{M} \{u^{(m)}\theta(Z^{(m)}, Z^{(m+1)}, \widehat{Z}^{(k)}) + v^{(m)}\lambda(Z^{(m)}, Z^{(m+1)}, \widehat{Z}^{(k)})\} \quad \text{for } k = 1, 2, \cdots, M+N. \tag{40}$$

From (14), (27) and (28), we find that

$$u^{(k)} = \sum_{p=1}^{M+N} c^{(kp)} w^{(p)} + h^{(k)}, \tag{41}$$

where

$$c^{(kp)} = -D^{(p)}(\rho^{(k)}, \zeta^{(k)})B^{(p)} + \sum_{n=1}^{M+N} D^{(n)}(\rho^{(k)}, \zeta^{(k)})L^{(p)}(\rho^{(n)}, \zeta^{(n)}) + \begin{cases} 1 & \text{if} \quad k = p \\ 0 & \text{if} \quad k \neq p \end{cases},$$

$$h^{(k)} = \sum_{m=1}^{M+N} D^{(m)}(\rho^{(k)}, \zeta^{(k)}) \frac{Q^{(m)}}{\sqrt{g^{(m)}}}. \tag{42}$$

Hence, (40) can be written as

$$\sum_{p=1}^{M+N} d^{(kp)} w^{(p)} + e^{(k)} = \frac{1}{2\pi} \sum_{m=1}^{M} v^{(m)} \lambda(Z^{(m)}, Z^{(m+1)}, \widehat{Z}^{(k)}) \quad \text{for } k = 1, 2, \cdots, M+N, \tag{43}$$

where

$$e^{(k)} = h^{(k)} - \frac{1}{2\pi} \sum_{m=1}^{M} h^{(m)} \theta(Z^{(m)}, Z^{(m+1)}, \widehat{Z}^{(k)}),$$

$$d^{(kp)} = c^{(kp)} - \frac{1}{2\pi} \sum_{m=1}^{M} c^{(mp)} \theta(Z^{(m)}, Z^{(m+1)}, \widehat{Z}^{(k)}). \tag{44}$$

The first boundary condition in (29) can be written as

$$w^{(k)} = p_1(\rho^{(k)}, \zeta^{(k)}) \text{ if } T \text{ is specified on } S^{(k)}. \tag{45}$$

The formula in (33) can be used to derive

$$\pi i F'(\widehat{Z}^{(k)}) = \sum_{m=1}^{M} (u^{(m)} + i v^{(m)}) \times [q(Z^{(m)}, Z^{(m+1)}, \widehat{Z}^{(k)}) + i r(Z^{(m)}, Z^{(m+1)}, \widehat{Z}^{(k)})] \quad \text{for } k = 1, 2, \cdots, M, \tag{46}$$

where q and r are real parameters defined by

$$q(a, b, c) + i r(a, b, c) = -\frac{1}{b - c} + \frac{1}{a - c}. \tag{47}$$

For further details, one may refer to Park and Ang [14].

With (46), the boundary condition on the second line of (29) and the one in (34) can be written as

$$\sum_{p=1}^{M+N} T^{(kp)} w^{(p)} - \sum_{m=1}^{M} Y^{(km)} v^{(m)} = X^{(k)} \text{ if } \frac{\partial T}{\partial n} \text{ is specified on } S^{(k)}, \tag{48}$$

where $T^{(kp)}$ are given by

$$T^{(kp)} = E^{(p)}(\rho^{(k)}, \zeta^{(k)}) + p_3(\rho^{(k)}, \zeta^{(k)}) c^{(kp)} + \sum_{m=1}^{M} c^{(mp)} R^{(km)}, \tag{49}$$

the coefficients $X^{(k)}$ are defined by

$$\begin{aligned} X^{(k)} = & -p_3(\rho^{(k)}, \zeta^{(k)}) h^{(k)} - \sum_{m=1}^{M} h^{(m)} R^{(km)} \\ & + \begin{cases} p_2(\rho^{(k)}, \zeta^{(k)}) & \text{if } S^{(k)} \text{ does not lie on } r = 0 \\ p_4(\rho^{(k)}, \zeta^{(k)}) & \text{if } S^{(k)} \text{ lies on } r = 0 \end{cases}, \end{aligned} \tag{50}$$

the real parameters $R^{(km)}$ and $Y^{(km)}$ are defined by

$$\begin{aligned} R^{(km)} + iY^{(km)} = & \frac{1}{\pi}(r(Z^{(m)}, Z^{(m+1)}, \widehat{Z}^{(k)}) - iq(Z^{(m)}, Z^{(m+1)}, \widehat{Z}^{(k)})) \\ & \times [n_z^{(k)} + in_r^{(k)}], \end{aligned} \tag{51}$$

and $[n_r^{(k)}, n_z^{(k)}]$ is the outward unit normal vector to $C^{(k)}$.

Equations (45) and (48) require the functions p_1, p_2 and p_3 to be evaluated at the midpoint $(\rho^{(k)}, \zeta^{(k)})$ of the boundary element $S^{(k)}$. According to (30), p_1, p_2 and p_3 are expressed in terms of f_1, f_2 and f_3 given by the boundary conditions in (7). Now, depending on the geometry of C, the midpoint $(\rho^{(k)}, \zeta^{(k)})$ may or may not lie on the actual physical boundary C. If $(\rho^{(k)}, \zeta^{(k)})$ does not lie on C, then the value of f_i $(i = 1, 2, 3)$ needed in the calculation of p_i at $(\rho^{(k)}, \zeta^{(k)})$ may be taken to be given by the average value of f_i at the endpoints of $S^{(k)}$, as the endpoints of every boundary element are chosen to lie on C.

We may solve (43) for $k = 1, 2, 3, \cdots, M+N$, together with (45), (48) and $v^{(M)} = 0$, as a system of $2M + N$ linear algebraic equations for the constants $w^{(p)}$ $(p = 1, 2, \cdots, M+N)$ and $v^{(m)}$ $(m = 1, 2, \cdots, M-1)$. Note that $v^{(M)}$ is set to zero to ensure that the imaginary part of the complex function $F(z + ir)$ is uniquely determined by the linear algebraic equations. It is assumed that T is specified on some part of C so that the temperature (hence the real part of $F(z + ir)$) is unique. The over-determined system of linear algebraic equations may be solved by using the method of least squares. Once the constants $w^{(p)}$ are found, $u^{(k)}$ can be computed from (41) and the required complex function $F(Z)$ is given by (37). Note that the value of the solution T at the collocation point $(\rho^{(k)}, \zeta^{(k)})$ is given $w^{(k)}/\sqrt{g(\rho^{(k)}, \zeta^{(k)})}$. The value of T at any other point in the solution domain can be approximately calculated from (31) and (37).

5 Specific problems

To assess its validity and accuracy, the complex variable boundary element procedure in Section 4 are applied to solve some specific problems.

Problem 1. Here the governing partial differential equation given by (1) and (2) with

$$g(r, z) = (r^2 + 1)^2,$$
$$Q(r, z) = \frac{\pi^2}{16}(r^2 + 1)^2 \cos(\frac{\pi}{4}z) - 12r^4 - 16r^2 - 4,$$

is to be solved in the domain as $0 < r < 1$, $0 < z < 1$, subject to

$$\left.\frac{\partial T}{\partial n}\right|_{z=0} = 0 \text{ for } 0 < r < 1,$$
$$\left.\frac{\partial T}{\partial n}\right|_{z=1} = -\frac{\pi\sqrt{2}}{8} \text{ for } 0 < r < 1,$$
$$T(1, z) = 1 + \cos(\frac{\pi}{4}z) \text{ for } 0 < z < 1.$$

As the solution domain contains points on $r = 0$, the complex variable boundary element procedure requires the additional condition

$$\left.\frac{\partial T}{\partial n}\right|_{r=0} = 0 \text{ for } 0 < z < 1.$$

In order to obtain some numerical results, the open boundary C and the line segment $r = 0$, $0 < z < 1$, are discretized into M equal length elements and N well spaced out collocation points are chosen inside the domain. In Table 1, three sets of numerical values of T are obtained by and compared with the exact solution

$$T(r, z) = r^2 + \cos(\frac{\pi}{4}z)$$

at 9 selected interior collocation points. Sets A, B and C are calculated using $(M, N) = (20, 9)$, $(M, N) = (40, 49)$ and $(M, N) = (80, 361)$ respectively. The average absolute errors of the numerical values of T at the selected points are given in the last row of Table 1. It is obvious that there is a significant improvement in the accuracy of the numerical values of T as M and N increases. The convergence rate is as may be expected since only constant elements are employed in the calculation here.

Table 1. Numerical and exact values of T at selected interior points.

(r, z)	Set A	Set B	Set C	Exact
$(0.25, 0.25)$	1.11764	1.05853	1.05241	1.04329
$(0.25, 0.50)$	1.25478	1.25205	1.24301	1.23079
$(0.25, 0.75)$	1.55035	1.57106	1.55906	1.54329
$(0.50, 0.25)$	1.01564	1.00502	0.99734	0.98638
$(0.50, 0.50)$	1.20628	1.19799	1.18763	1.17388
$(0.50, 0.75)$	1.52317	1.51689	1.50359	1.48638
$(0.75, 0.25)$	0.91183	0.90878	0.90275	0.89397
$(0.75, 0.50)$	1.11442	1.10213	1.09327	1.08147
$(0.75, 0.75)$	1.43680	1.42092	1.40921	1.39397
Average absolute error	0.03306	0.02100	0.01191	-

Problem 2. The governing partial differential equation is given by (1) and (2) with

$$g(r, z) = z + 1,$$
$$Q(r, z) = -4z - 6.$$

It is to be solved in a concave solution domain, specifically the one sketched in Figure 2. Note that the curved part of the boundary of the solution domain is defined by $(r-2)^2 + (z-2)^2 = 1$, $1 < r < 2$, $1 < z < 2$.

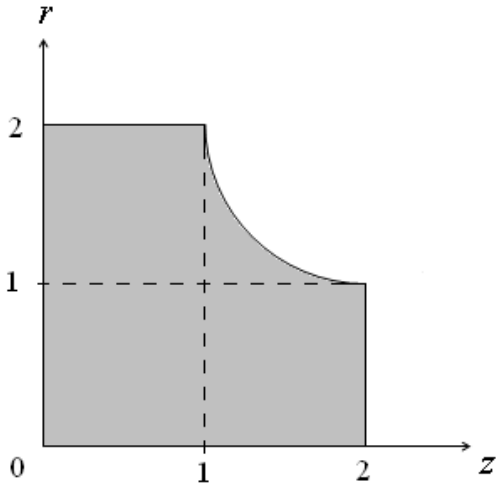

Figure 2. Solution domain for Problem 2.

The boundary condtitions of the problem are

$$\left.\frac{\partial T}{\partial n}\right|_{z=2} = 2 \text{ for } 0 < r < 1,$$
$$\frac{\partial T(r,z)}{\partial n} = 2r(r-2) + 2(z-2)$$
$$\text{for } (r-2)^2 + (z-2)^2 = 1, 1 < r < 2,\ 1 < z < 2,$$
$$T(2,z) = 4 + 2z \text{ for } 0 < z < 1,$$
$$T(r,0) = r^2 \text{ for } 0 < r < 2.$$

For the purpose of obtaining some numerical results, the curved part of the boundary is discretized into $2N_0$ elements, each of the straight parts given by $r = 0,\ 0 < z < 2$ and $z = 0,\ 0 < r < 2$ into $2N_0$ elements, and each of the remaining parts given by $r = 2,\ 0 < z < 1$ and $z = 2,\ 0 < r < 1$ into N_0 elements. Thus, the total number of elements is given by $M = 8N_0$. The interior collocation points are chosen to be evenly distributed inside the solution domain.

The normal derivative of the temperature (that is, the heat flux) is specified on the curve part of the boundary. We compare the numerically computed temperature on the semi-circle with the exact temperature given by

$$T(r,z) = r^2 + 2z.$$

Figure 3 gives plots of the numerical and exact temperature against the angle $\theta = \arctan(r/z)$ for $(r-2)^2 + (z-2)^2 = 1, 1 < r < 2,\ 1 < z < 2$. The two plots obtained by using 192 boundary elements ($N_0 = 24$) and 419 interior collocation points are in good agreement with each other.

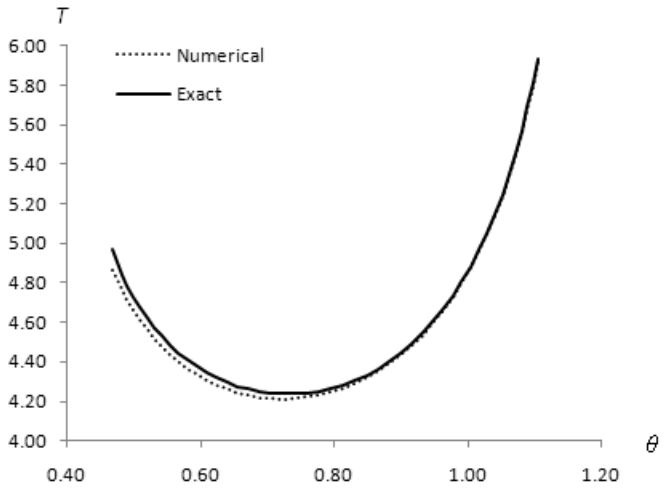

Figure 3. Plots of numerical and exact temperature on the curved part of the boundary.

The normal heat fux $g\partial T/\partial n$ on $r = 2, 0 < z < 1$ is not known a priori (from the boundary conditions of the problem). It can be calculated directly from the complex variable boundary element solution. In Figure 4, the numerically calculated normal heat flux on $r = 2, 0 < z < 1$ is plotted against z and compared with the one computed from the exact solution. The numerical and the exact values of the flux show good agreement with each other, except at points near the sharp corners $(2, 0)$ and $(2, 1)$ where there is a loss in the accuracy of the numerical calculation. Nevertheless, at any fixed point near a sharp corner point, further calculations show that the accuracy of the numerical flux can be improved significantly by employing more elements near the corner.

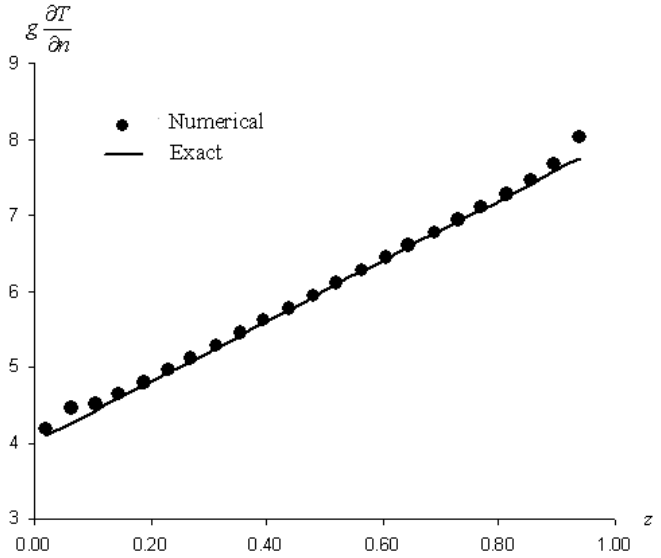

Figure 4. Plots of numerical and exact flux on $r = 2$, $0 < z < 1$.

Problem 3. Take the solution domain to be $1 < r < 2, 1 < z < 2$ (a hollow cylinder) and the function g and Q in (1) and (2) to be given by

$$g(r, z) = r + z,$$
$$Q(r, z) = -\frac{1}{r} - 1.$$

The governing partial differential equation is to be solved in the solution domain subject to the boundary conditions

$$\left.\frac{\partial T}{\partial n}\right|_{r=1} = -1 \text{ for } 1 < z < 2,$$
$$\left.\frac{\partial T}{\partial n}\right|_{r=2} = \frac{1}{2} \text{ for } 1 < z < 2,$$
$$T(r, 1) = 1 + \ln r \text{ for } 1 < r < 2,$$
$$T(r, 2) = 2 + \ln r \text{ for } 1 < r < 2.$$

To obtain some numerical results, each side of the square solution domain in the rz plane is discretized into M_0 equal length elements. The interior

collocation points are chosen as $(1 + j/M_0, 1 + k/M_0)$ for $j = 1, 2, \cdots, M_0 - 1$ and $k = 1, 2, \cdots, M_0 - 1$, so the total interior collocation points are $N = (M_0 - 1)^2$. In Table 2, numerical values of T at selected interior points, which are obtained using $M_0 = 4$, 12 and 24, are compared with the exact solution

$$T(r, z) = z + \ln r.$$

There is an obvious reduction in the average absolute error of the numerical values at the selected interior points when the calculation is refined using larger M_0. The average absolute error for $M_0 = 4$ is two and the half times larger than that for $M_0 = 12$, and the average absolute error for $M_0 = 12$ is twice as large as that for $M_0 = 24$.

Table 2. Numerical and exact values of T at selected interior points.

(r, z)	$M_0 = 4$	$M_0 = 12$	$M_0 = 24$	Exact
$(1.25, 1.25)$	1.43249	1.46465	1.46904	1.47314
$(1.25, 1.50)$	1.63930	1.64889	1.65221	1.65547
$(1.25, 1.75)$	1.79015	1.80422	1.80694	1.80962
$(1.50, 1.25)$	1.71717	1.72041	1.72183	1.72314
$(1.50, 1.50)$	1.90420	1.90527	1.90535	1.90547
$(1.50, 1.75)$	2.05984	2.06070	2.06013	2.059616
$(1.75, 1.25)$	1.98831	1.97740	1.97520	1.973144
$(1.75, 1.50)$	2.16944	2.16182	2.15856	2.15547
$(1.75, 1.75)$	2.34167	2.31680	2.31312	2.30962
Average absolute error	1.61×10^{-2}	0.61×10^{-2}	0.31×10^{-2}	-

Problem 4. Consider a solid cylinder that occupies the region $0 < r < L$, $0 < z < L$, where L is a positive constant. The thermal conductivity κ of the solid varies in the z direction as $\kappa = \kappa_0(1 + \alpha z)^2$, where κ_0 and α are positive constants.

It is assumed that there is no internal heat generation in the cylindrical solid, that is, $Q = 0$. A portion of the cylindrical surface at $z = 0$ is subject to heating with uniform flux q_0, while the cylindrical surface at $z = 1$ has heat removed by the convection process. The remaining cylindical surface is thermally insulated. More precisely, the boundary conditions are given by

$$\begin{aligned}
\kappa\frac{\partial T}{\partial n} &= h_{\text{amb}}(T_{\text{amb}} - T) \text{ for } 0 < r < L,\ z = L,\\
\kappa\frac{\partial T}{\partial n} &= 0 \text{ for } 0 < z < L,\ r = L,\\
\kappa\frac{\partial T}{\partial n} &= 0 \text{ for } L/2 < r < L,\ z = 0,\\
\kappa\frac{\partial T}{\partial n} &= q_0 \text{ for } 0 < r < L/2,\ z = 0,
\end{aligned}$$

where h_{amb} and T_{amb} are the ambient heat convection coefficient and ambient temperature respectively.

To compute the non-dimensionalized temperature $\kappa_0(T - T_{\text{amb}})/(q_0 L)$ using the complex variable boundary element method (CVBEM) here, the exterior boundary of the cylindrical solid on the axisymmetric coordinate plane is discretized into $3N_0$, and $(N_0 - 1)^2$ well distributed interior collocation points are chosen. As the solution domain contains points on the z axis, the CVBEM procedure requires the line segment $0 < z < L$, $r = 0$, to be discretized into elements. It (the line segment) is divided up into N_0 elements. For comparison, numerical values of $\kappa_0(T - T_{\text{amb}})/(q_0 L)$ are also obtained by using the axisymmetric boundary element method (A-BEM) with discontinuous linear elements as described in Yun and Ang [16].

Table 3. Numerical values of $\kappa_0(T - T_{\text{amb}})/(q_0 L)$.

	$N_0 = 8$		$N_0 = 16$		$N_0 = 20$	
$(r/L, z/L)$	CVBEM	A-BEM	CVBEM	A-BEM	CVBEM	A-BEM
$(0.25, 0.25)$	0.25290	0.24883	0.25087	0.24880	0.25044	0.24880
$(0.25, 0.50)$	0.19919	0.19993	0.20007	0.19993	0.20009	0.19993
$(0.25, 0.75)$	0.15342	0.15686	0.15572	0.15688	0.15601	0.15688
$(0.50, 0.25)$	0.14558	0.14515	0.14555	0.14515	0.14549	0.14515
$(0.50, 0.50)$	0.12652	0.12776	0.12748	0.12776	0.12758	0.12776
$(0.50, 0.75)$	0.10942	0.11190	0.11105	0.11191	0.11127	0.11191
$(0.75, 0.25)$	0.07174	0.07260	0.07236	0.07260	0.07244	0.07260
$(0.75, 0.50)$	0.06535	0.06674	0.06631	0.06674	0.06643	0.06674
$(0.75, 0.75)$	0.05919	0.06129	0.06054	0.06129	0.06074	0.06129

For $\alpha L = 1/10$, the numerical values of $\kappa_0(T - T_{\text{amb}})/(q_0 L)$ at selected interior points, obtained using the CVBEM and the A-BEM with $N_0 = 8$, 16 and 20, are given in Table 3. It is obvious that the CVBEM and A-BEM solutions approach each other as N_0 increases. Note that only constant elements are used in the CVBEM. Thus, as expected, the convergence rate of the CVBEM solution is slower than that of the linear element A-BEM.

On the plane $0 < r/L < 1$, $z/L = 0$, where the surface heating occurs, the temperature is not known a priori. We plot the non-dimensionalized temperature $\kappa_0(T - T_{\text{amb}})/(q_0 L)$ against r/L on the surface $0 < r/L < 1$, $z/L = 0$, for selected values of the non-dimensionalized parameter αL in Figure 5. The plots in Figure 5 are obtained using the CVBEM and the A-BEM with $N_0 = 16$. The numerical values of the surface temperature calculated using the CVBEM are in close agreement with those obtained using the A-BEM. The temperature is lower if αL has a larger value. This is to be expected, as the solid conducts heat away better from where the surface heating occurs if the thermal conductivity $\kappa = \kappa_0(1 + \alpha z)^2$ is larger.

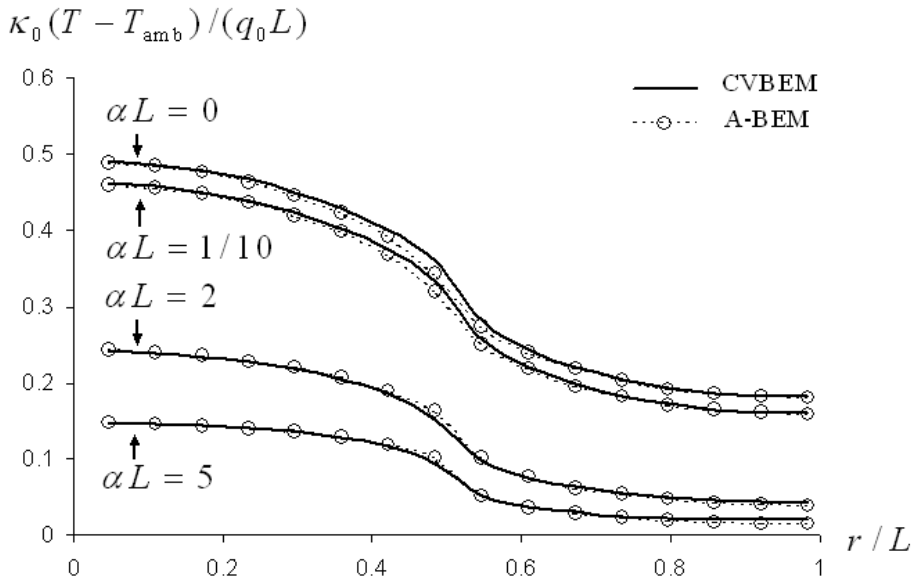

Figure 5. Plots of $\kappa_0(T - T_{\text{amb}})/(q_0 L)$ against r/L on the surface $0 < r/L < 1$, $z/L = 0$.

6 Summary

The problem of axisymmetric steady-state heat conduction problem in a non-homogeneous isotropic solid is considered here. The problem is reformulated approximately as one governed by the two-dimensional Laplace's equation to be solved by constructing a suitable analytic complex function. The Cauchy integral formula and its differentiated form are used to reduce the numerical construction of the analytic function to solving a system of linear algebraic equations. The numerical procedure does not require the solution domain to be divided into small elements. Only the boundary is discretised into straight line elements.

To assess its validity and accuracy, the proposed complex variable boundary element procedure is applied to solve some specific cases of the axisymmetric heat conduction problem. In all the cases, the numerical solutions

obtained agree favourably with known solutions and convergence in the numerical values obtained is observed when the number of boundary elements and interior collocation points is increased. This suggests that the complex variable boundary element formulation presented here is correctly derived and it can be used as an accurate and reliable tool for the analysis of the axisymmetric heat conduction problem.

References

[1] W. T. Ang, Numerical solution of a linear elliptic partial differential equation with variable coefficients: a complex variable boundary element approach, *Numerical Methods for Partial Differential Equations* (in press). http://dx.doi.org/10.1002/num.20667.

[2] W. T. Ang and D. L. Clements, A boundary element method for determining the effect of holes on the stress distribution around a crack, *International Journal for Numerical Methods in Engineering* **23** (1986) 1727-1737.

[3] W. T. Ang, D. L. Clements and N. Vahdati, A dual-reciprocity boundary element method for a class of elliptic boundary value problems for nonhomogeneous anisotropic media, *Engineering Analysis with Boundary Elements* **27** (2003) 49-55.

[4] C. A. Brebbia and J. Dominguez, Boundary element methods for potential problems, *Applied Mathematical Modelling* **1** (1977) 372-378.

[5] C. A. Brebbia and D. Nardini, Dynamic analysis in solid mechanics by an alternative boundary element procedure, *International Journal of Soil Dynamics and Earthquake Engineering* **2** (1983) 228-233.

[6] C. A. Brebbia, J. C. F. Telles and L. C. Wrobel, *Boundary Element Techniques, Theory and Applications in Engineering*, Springer-Verlag, Berlin/Heidelberg, 1984.

[7] D. L. Clements, M. Haselgrove and M. D. Barnett, A note on the boundary integral method for the solution of second order elliptic equations, *Journal of Australian Mathematical Society Series B* **26** (1985) 415-421.

[8] J. T. Chen and Y. W. Chen, Dual boundary element analysis using complex variables for potential problems with or without a degenerate boundary, *Engineering Analysis with Boundary Elements* **24** (2000) 671-684.

[9] J. T. Chen and H.-K. Hong, Review of dual boundary element methods with emphasis on hypersingular integrals and divergent series, *Applied Mechanics Reviews* **52** (1999) 17-33.

[10] A. A. Dobroskok and A. M. Linkov, CV dual reciprocity BEM for transient flow in blocky systems with singular points and lines of discontinuities, *Engineering Analysis with Boundary Elements* **34** (2010) 238-247.

[11] H.-K. Hong and J. T. Chen, Derivations of Integral Equations of Elasticity, *Journal of Engineering Mechanics* **114** (1988) 1028-1044.

[12] T. V. Hromadka II and C. Lai, *The Complex Variable Boundary Element Method in Engineering Analysis*, Springer-Verlag, Berlin, 1987.

[13] E. H. Ooi, W. T. Ang and E. Y. K. Ng, A boundary element model of the human eye undergoing laser thermokeratoplasty, *Computers in Biology and Medicine* **38** (2008) 727-737.

[14] Y. S. Park and W. T. Ang, A complex variable boundary element method for an elliptic partial differential equation with variable coeffi-

cients, *Communications in Numerical Methods in Engineering* **16** (2000) 697-703.

[15] F. J. Rizzo, An integral equation approach to boundary value problems of classical elastostatics, *Quarterly of Applied Mathematics* **25** (1967) 83-95.

[16] B. I. Yun and W. T. Ang, A dual-reciprocity boundary element approach for axisymmetric nonlinear time-dependent heat conduction in a nonhomogeneous solid, *Engineering Analysis with Boundary Elements* **34** (2010) 697-706.